Variable circumstellar structure of luminous hot stars: the impact of spectroscopic long-term campaigns

Andreas Kaufer

Landessternwarte Heidelberg
Königstuhl 12
D-69117 Heidelberg, Germany
email: A.Kaufer@lsw.uni-heidelberg.de

Abstract

An extensive spectroscopic long-term monitoring program was carried out by the Landessternwarte Heidelberg to examine the variable circumstellar structure of different classes of luminous hot stars. The observations made use of a portable fiber-linked echelle spectrograph named FLASH/HEROS, which was developed for this purpose and was mostly mounted to small to medium-size telescopes at different observing sites. Over 8 years, more than 12 000 science spectra could be collected in about 900 nights, which builds a to date unprecedented data base of spectroscopic time series of variable hot stars with high resolution in wavelength and time. In this contribution, some of the highlights of the astronomical results obtained from these extended observing campaigns will be reported with particular emphasis on the new insights gained in the physical mechanisms causing the variability of the circumstellar envelopes.

1 Introduction

The hot-star group of the Landessternwarte Heidelberg is primarily working on the variability of luminous hot stars like Luminous Blue Variables (LBVs, B. Wolf, O. Stahl, Th. Szeifert, A. Kaufer), Wolf-Rayet stars (J. Schweickhardt in collaboration with W. Schmutz, Zürich), OBA hyper- and supergiants (A. Kaufer, Th. Rivinius, D. Schäfer, O. Stahl, B. Wolf), and Be stars (Th. Rivinius in collaboration with D. Baade, ESO, and S. Štefl, Ondrejov).

The hot stars' variability, which is present all-over the upper HR-diagram, is used to develop new and refined pictures of the stars' envelope and photosphere structures. The variability provides a natural laboratory to examine and understand the physical mechanisms acting in the extended and highly structured atmospheres. Our most extensively used observational tool for this research is the long-term monitoring of the stellar variability with high resolution in wavelength and time with dedicated spectroscopic instruments at small to medium-size telescopes.

In this 'highlight' contribution I will first derive the observational requirements posed by the objects under examination. Then, the FLASH/HEROS instrument developed for this special purpose and the major observing campaigns will be shortly described. Finally, I will report on the highlights of the astronomical results from these extended observing

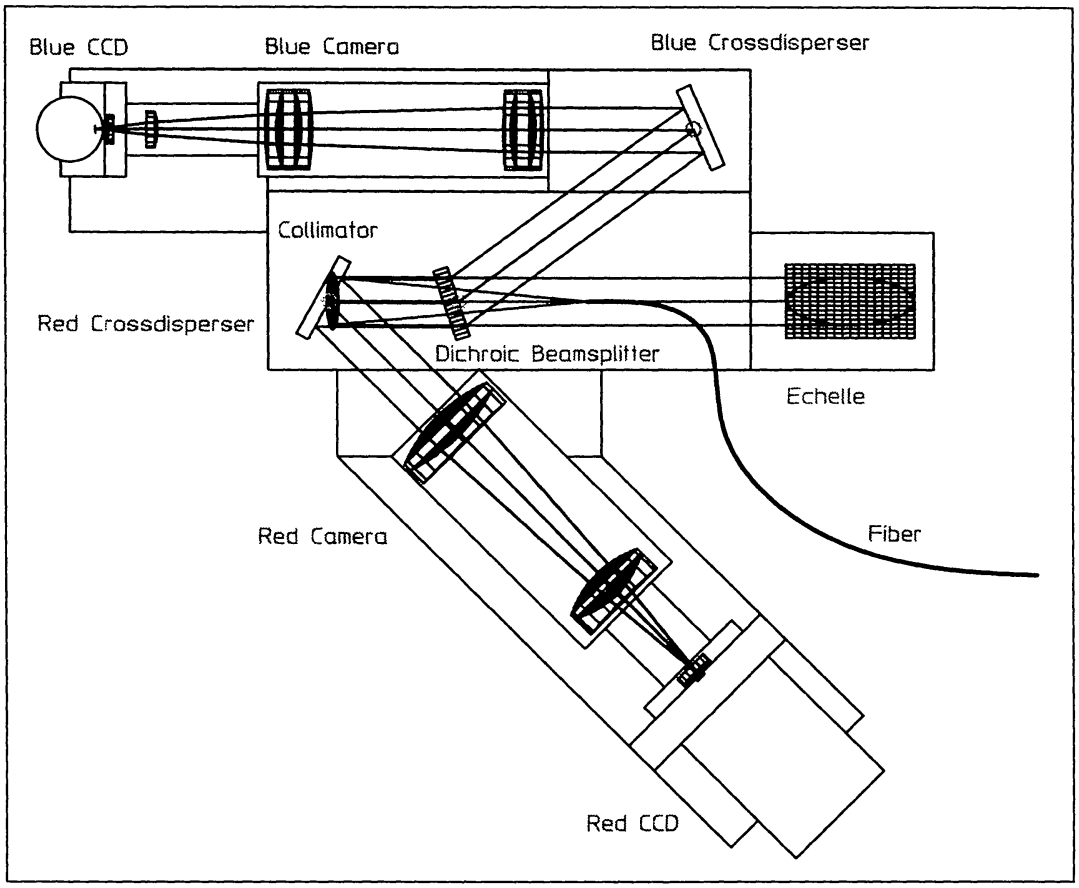

Figure 1: HEROS optical layout: the beam coming from the fiber is collimated on the echelle grating, the dispersed beam is then split by a dichroic filter and fed simultaneously to the 'red' and 'blue' channels, both equipped with individually adapted crossdisperser gratings, dioptric cameras, and CCD detectors.

campaigns with emphasis on the new insights gained for the variability mechanisms of the circumstellar envelopes of the examined objects.

2 Variability of luminous hot stars

Basically all classes of luminous hot stars are well known to be photometrically and spectroscopically variable. The velocity fields in the atmospheres of these objects exhibit very complex patterns due to phenomena like spherical radiation-driven winds, non-spherical outflow and infall, (co-)rotating circumstellar material in the envelopes, large- and small-scale magnetic fields, but also radial and non-radial pulsations and rotation in the stellar photospheres. In addition, the effects of the always underlying stellar rotation has to be considered. The absolute velocities involved span a large range from $< 1\,\mathrm{km\,s^{-1}}$ in the photospheres up to several hundreds to thousands of $\mathrm{km\,s^{-1}}$ in the supersonic outflows. Also the time scales corresponding to the different mechanisms of the variability span a large dynamical range from several hours to several months. In most cases the time scales are observed to be multiple, indicating that in general not a single mechanism can be made responsible for the observed variability.

In principle, the time-dependent stellar line-profile variations (LPVs) contain the necessary information to identify the underlying physical mechanisms. Since selected spectral lines emerge from different layers of the star's atmosphere, also information on the depth dependence of the acting mechanisms is present. This gives us the exciting perspective to tackle the question about the causal physical connection of the stellar photosphere and interior with the stellar envelope and its variability and to eventually overcome the highly artificial separation between a star and its envelope. In practice, of course, the inversion or modeling of the observational data will not always lead to an unequivocal picture of the whole extended atmosphere but surely is one of the most powerful tools for this kind of studies.

The adequate observation of the time-dependent LPVs poses high demands on the required spectroscopic instruments and observing sites: a high spectral resolving power of $R \gtrsim 20\,000$ is needed to follow the general evolution of the line profiles or any discrete features in the line profiles; a large wavelength range from near UV to near IR is needed to cover simultaneously spectral lines emerging from different layers of the star's atmosphere, i.e., from the photosphere throughout the envelope; a long time base of months and a good time resolution of $\lesssim 1$ day is crucial to causally connect the observed phenomena and to provide the input for a quantitative time-series analysis.

Entrance aperture: $100 - 300\,\mu$m

Fiber: 10 m length, $100\,\mu$m core diameter + entrance micro lens ($f/15 \rightarrow f/4.5$)

Collimator: $f/4.5$, $f = 360$ mm

R2 Echelle grating: 31.6 grooves/mm, blaze angle= 63.4°

Dichroic beam splitter: edge wavelength = 5700 Å

Red Channel (= FLASH)**:**

- **Cross disperser:** 300 grooves/mm, blaze wavelength = 5000 Å
- **Camera:** $f/2.8$, $f = 300$ mm
- **CCD:** EEV 1152 × 770, 22 μm pixel, LN_2 cooled

Blue Channel (detachable):

- **Cross disperser:** 400 grooves/mm, blaze wavelength = 3900 Å
- **Camera:** $f/2.8$, $f = 300$ mm, transmission > 80% down to 3500 Å
- **CCD:** EEV 1170 × 800, 22 μm pixel, LN_2 cooled; in 1996 replaced by a thinned, back-illuminated SiTE 2000 × 800 pixel CCD, 15 μm pixels, LN_2 cooled

Table 1: HEROS system data. To the original instrument named FLASH (Mandel 1988) which basically consisted of the 'red' channel only, the 'blue' channel was added in early 1995 to access the wavelength range below 4000 Å. A microlens to re-image the entrance aperture in the telescope's focal plane on the fiber core and to adapt the telescopes' f-ratios to a f-ratio well-suited for the fiber was introduced in early 1997.

3 The FLASH/HEROS instrument

These observational requirements are difficult to meet with the instrumentation offered at most of the astronomical observatories. High-resolution spectrographs are commonly offered at the largest telescopes only, which cannot be used for continuous observing runs of several months length. On the other hand, basically all classes of the most luminous stars have some bright prototypes in the reach of even the smallest telescopes. Therefore, high-resolution spectroscopy at small to medium-size telescopes is needed for variability studies of hot luminous stars.

To fulfill the instrumental requirements, a portable fiber-linked echelle spectrograph first named FLASH, the **F**iber-**L**inked **A**stronomical **S**pectrograph of **H**eidelberg (Mandel 1988) later extended to HEROS, the **H**eidelberg **E**xtended **R**ange **O**ptical **S**pectrograph, was developed and built at the Landessternwarte. Figure 1 displays the optical layout of the HEROS spectrograph, Table 1 gives further details on the system components. HEROS provides a resolving power of $R = \lambda/\Delta\lambda \approx 20\,000$ over the complete optical wavelength range from 3500 to 8600 Å in two channels (blue: $3450 - 5600$ Å, red: $5800 - 8650$ Å). Both channels are equipped with individually adapted grating crossdispersers, dioptric cameras and sensitive CCD detectors and can be exposed simultaneously. Due to the fiber link, the HEROS spectrograph only needs a light-weight fiber-entrance module which carries the guiding and calibration unit (a halogen lamp for flatfielding and a Thorium-Argon hollow-cathode lamp for wavelength calibration) and can be mounted even to the smallest telescopes of the sub-meter class where long and continuous observing runs can be carried out over periods of months. Due to limitations on the size and budget of the spectrograph, the total efficiency is only about 1.5% but allows to reach a $S/N \approx 100$ in 1 hour with a 50-cm telescope for a 6^{th} magnitude star. The bench-like mounting of the HEROS instrument provides a high long-term stability of the spectral format with a radial-velocity accuracy of $< 0.5\,\mathrm{km\,s^{-1}}$ which is crucial for long-term programs.

4 25 000 spectra in 935 nights – the long-term campaigns from 1990–1997

The first long observing campaign carried out with the original FLASH spectrograph was dedicated to the spectral variations of the LBV prototype P Cygni and the prototypical A-type supergiant α Cygni and made use of the 70-cm telescopes of the Landessternwarte Heidelberg, the 1.23-m telescope on Calar Alto Observatory and the 2-m telescope of the Landessternwarte Tautenburg from 1990 to 1992. Stahl et al. (1994) report on the first promising results obtained on P Cygni where for the first time the medium-term and micro-variability could be spectroscopically followed on times scales from weeks to months.

In the following years from 1992 to 1997 more than 600 nights in blocks of 60 to 120 nights were spent with the FLASH and HEROS instruments mainly on the ESO 50-cm telescope at the La Silla observatory in Chile. Due to the excellent weather conditions at this site and the high availability of the otherwise purely photometric telescope, a time resolution of one spectrum per night over several months was obtained for most of the bright (< 7 mag) program stars (see also Wolf et al. 1993).

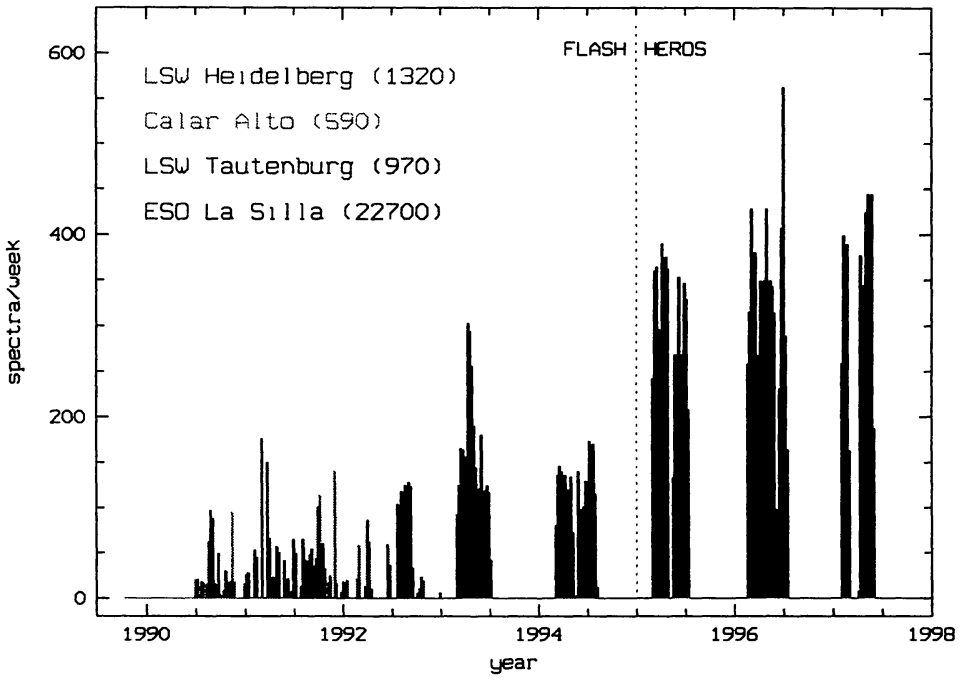

Figure 2: Histogram of raw spectra obtained per week over the years from 1990 to 1997 with the FLASH and after 1995 with the HEROS spectrographs. The numbers in parentheses give the total number of spectra obtained per observatory. In Heidelberg the 70-cm telescopes were used, at Calar Alto the 1.23-m and the 2.2-m, in Tautenburg the 2-m, and at ESO La Silla the ESO 50-cm, the Bochum 60-cm, and the ESO 1.52-m telescopes.

In total more than 25 000 raw spectra were collected by 21 different observers in 935 observing nights over the years from 1990 to 1997 (cf. Fig. 2). This large amount of raw data is homogeneously reduced in a semi-automatic echelle-reduction software package implemented in the MIDAS (Munich Image Data Analysis System, ESO) environment and results in about 12 000 fully reduced one-dimensional science spectra. Some data sets of selected objects are published on CD-ROM by Stahl et al. (1995) who also describe the reduction process in detail; on request, all data material published in refereed journals is made available by the respective authors.

5 The highlights of the results

In this section I will report on some of the highlights of the results from these extended observing campaigns with some emphasis on the new insights gained for the variability mechanisms of the circumstellar envelopes of the peculiar main-sequence O star θ^1 Ori C, the extreme early-B hypergiant ζ^1 Sco, some late-B and early-A supergiants, and the Be star μ Cen.

5.1 The first O-type MS star identified as an oblique magnetic rotator: θ^1 Ori C (O7 V)

θ^1 Ori C (= HD 37022) is the visually brightest and hottest star of the Trapezium in the Orion nebula (M 42). It is a very young main sequence O star of the spectral type O7 V and therefore is the main source of ionizing photons of this nebula. Conti (1972) and Walborn (1981) discovered some spectroscopic peculiarities already a long time ago.

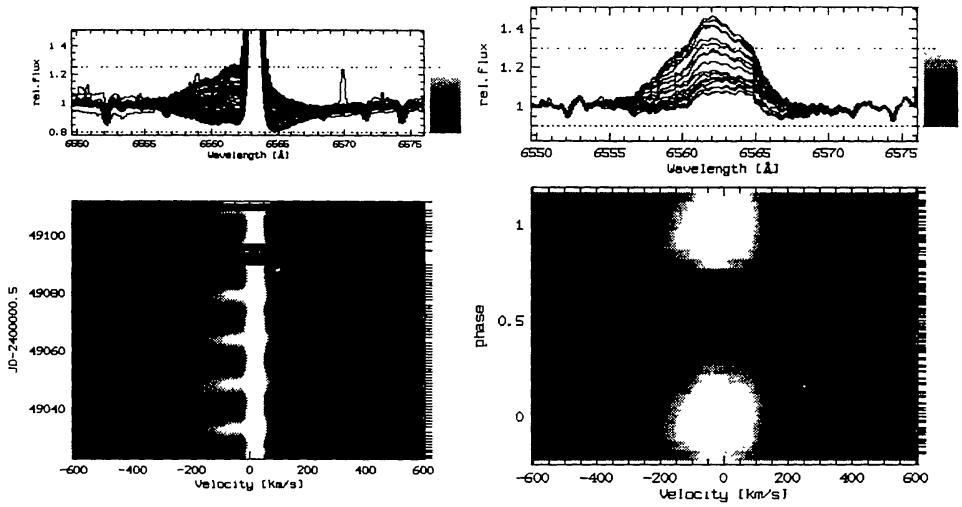

Figure 3: Dynamical spectrum of the Hα-line of θ^1 Ori C as from the discovery in 1993 (left). The strong sharp emission at the line center is due to the emission of the Orion nebula. The nebular emission peak and the underlying stellar absorption profile were removed for the dynamical phase spectrum on the right-hand side, which includes all spectra taken in the years from 1992 to 1995 folded with a period of 15.422 days. The maximum emission-line strength is defined as phase $\phi = 0$. Note that the major part of the variability is caused by blue-shifted emission with its maximum strength at this phase but also a weak red emission is discernible at $\phi = 0.5$.

Surprisingly, the first extended monitoring of θ^1 Ori C with FLASH in 1993 revealed an obvious, strictly periodic, and strong modulation of the Hα and HeIIλ4686 emission lines with a period of 15.4 days (Stahl et al. 1993). Figure 3 shows these periodic variations of the Hα-line profile as dynamical spectra and indicates that the major contribution to the variability comes from a blue-shifted emission component in the lines.

In early 1995, simultaneous spectral times series were obtained with the IUE space observatory and the just commissioned HEROS spectrograph over one cycle which now allowed to phase 15 years of IUE archival spectra with the ground based optical spectra. With this long time base of about 400 cycles the modulation period of θ^1 Ori C could be determined very precisely to $P = 15.422 \pm 0.002$ days. Further it was found that in addition to the UV wind lines and the optical emission lines, all strong photospheric lines exhibit a modulation of their equivalent widths with the same period. In the three panels of Fig. 4 the phase relation of the UV wind lines, the optical emission lines, and the photospheric lines is shown: it is found that the UV wind lines show excess wind absorption at $\phi = 0.5$ whereas the maximum strength of the optical emission lines coincides with the maximum absorption of the photospheric lines at $\phi = 0.0$.

From these phase-resolved optical and UV observations, an oblique magnetic rotator model (cf. Fig. 5) was proposed to explain the phase-locked photospheric and stellar-wind

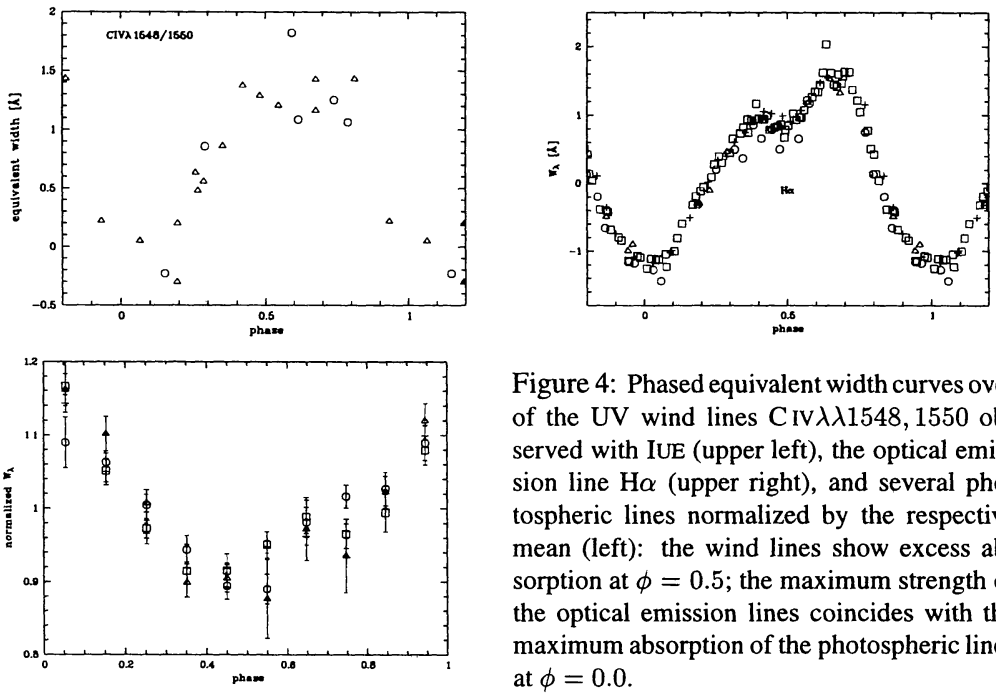

Figure 4: Phased equivalent width curves over of the UV wind lines C IV$\lambda\lambda$1548, 1550 observed with IUE (upper left), the optical emission line Hα (upper right), and several photospheric lines normalized by the respective mean (left): the wind lines show excess absorption at $\phi = 0.5$; the maximum strength of the optical emission lines coincides with the maximum absorption of the photospheric lines at $\phi = 0.0$.

variations of θ^1 Ori C (Stahl et al. 1996). We have strong observational evidence that the driving clock of the variability is the stellar rotation which forces the circumstellar envelope to rotation by an extended magnetosphere. This quite naturally explains that the excess absorption at highly blue-shifted velocities in the UV wind lines originates from the region above the magnetic pole with its fast wind; on the other hand, the excess emission of optical lines comes from an extended region of magnetically trapped gas of enhanced density near the magnetic equator. The excess absorption in the photospheric lines spatially coincides with the emission region and – since the relative amplitude of the modulation is independent of the ionic species of the photospheric lines – cannot be understood in terms of local chemical peculiarities or temperature effects but must be attributed to a disturbed atmospheric structure in this localized region.

Based on the 15.422-day period, well-aimed ROSAT observations were carried out by Gagné et al. (1997) who detected that the X-ray emission varies also in phase with the optical emission lines. Babel and Montemerle (1997) could quantitatively explain the X-ray flux and its variations with a "magnetically confined wind shock" model which gives further strong support for a magnetic origin of the variability. Therefore, θ^1 Ori C seems to be closely related to the cooler He-variable magnetic stars but is so far unique among the O-type stars.

5.2 The expanding atmosphere of the early B hypergiant ζ^1 Sco.

Early-B hypergiants belong to the most luminous stars ($M_{\rm bol} \approx -10 \ldots -11$ mag) in the Universe. Their spectra are distinguished by strong P Cygni-type profiles of H I and He I lines indicating a strong mass loss of the order of $10^{-5} M_\odot {\rm yr}^{-1}$. The best-investigated early-B hypergiant is the prototype ζ^1 Sco (= HD 152236, B1.5 Ia$^+$, $M_{\rm v} \approx -9$ mag) which is a member of the Sco OB1 association. ζ^1 Sco has been well-known for a long time to exhibit various kinds of photometric and spectroscopic variations on time

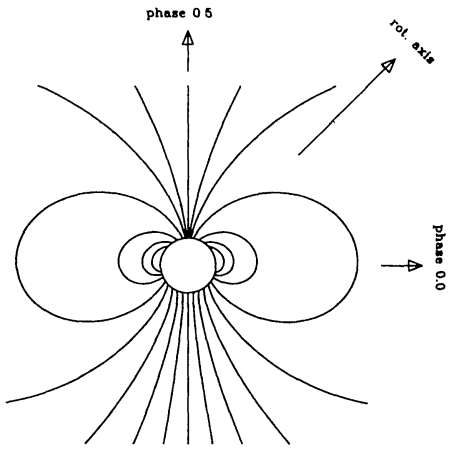

Figure 5: Sketch of the oblique magnetic rotator model for θ^1 Ori C: it is assumed that both the inclination between the magnetic and rotational axis and the inclination of the rotation axis to the line of sight are 45°. Then at $\phi = 0.5$ the magnetic pole with a fast wind observable as deepened blue absorptions in the UV wind lines comes into view, whereas at $\phi = 0.0$ the observer sees the magnetic equator where a dense emission region is to be located. A strong quadrupole contribution has been assumed to produce this magnetic field geometry and helps to explain the blue-shift of the optical emission lines originating in the therefore asymmetric equator region.

scales of about two weeks with amplitudes of 0.1 mag in brightness and $20\,\mathrm{km\,s^{-1}}$ in radial velocities (cf. e.g. Sterken 1977, Sterken & Wolf 1978). Asymmetric blue wings extending to -200 to $-300\,\mathrm{km\,s^{-1}}$ in practically all optical lines indicate that no lines in this extreme object are formed in a pure hydrostatic photosphere but in an expanding atmosphere (Wolf & Appenzeller 1979).

The outward accelerating stellar wind of ζ^1 Sco is well-documented in many P-Cygni lines in the optical and UV spectrum. The HEROS long-term campaigns now for the first time allowed to follow the time evolution of the variations of the expanding envelope (Rivinius et al. 1997a). Discrete absorption components (DACs) as best-known from the numerous UV observations of many other luminous hot stars are found for ζ^1 Sco in the optical P-Cygni wind profiles (cf. Fig. 6). These DACs indicate outward accelerating

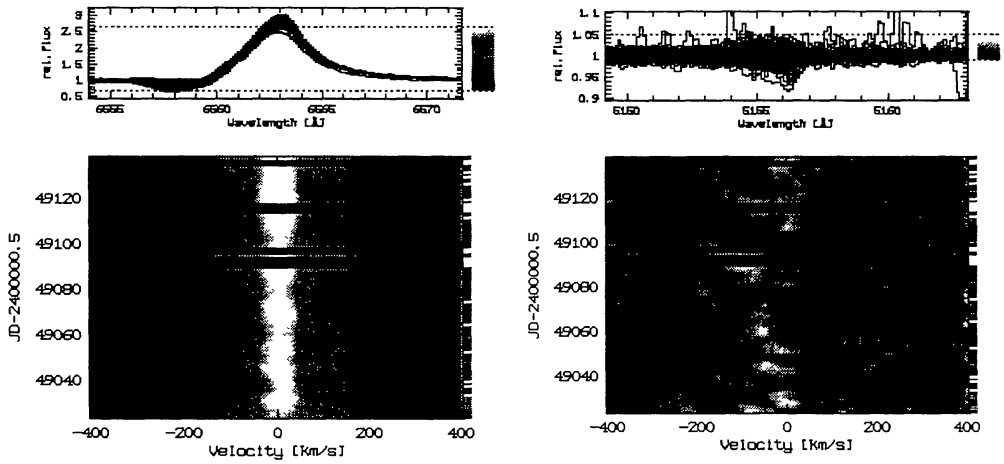

Figure 6: Dynamical spectra of the strong P Cyg-type wind line Hα line (left) and the much weaker but also wind-sensitive Fe IIIλ5156 line (right) observed in the B-type hypergiant ζ^1 Sco in 1993. Four individual discrete absorption components (DACs) could be precisely traced in these time series which extend over about 120 nights of observation with a sampling of one spectrum per night.

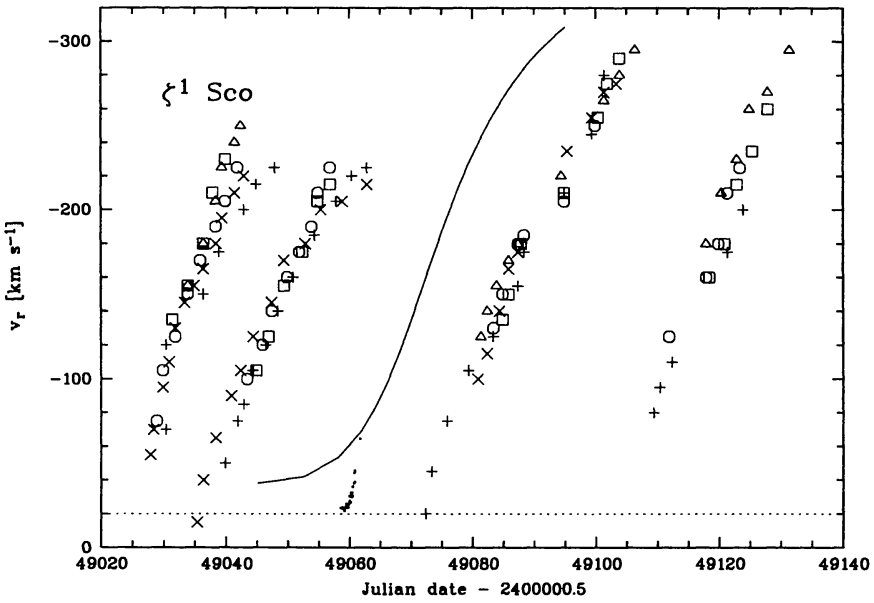

Figure 7: The acceleration of the discrete absorption features through the ambient wind. The symbols refer to the lines used to trace the DACs: Fe IIIλ5127 (+), Fe IIIλ5156 ($\times$), He Iλ6678 ($\circ$), He Iλ5876 ($\square$), Hα ($\triangle$). A velocity law with $\beta = 2.5, v_\infty = -370\,\mathrm{km\,s^{-1}}$, and $v_{\mathrm{sys}} = -20\,\mathrm{km\,s^{-1}}$ has been superimposed to demonstrate the slow and almost constant acceleration of the DACs over a large velocity range. Together with the velocity law observed in the photospheric lines (Fig. 9) which is overplotted here with small dots, a strong discrepancy between the often-used β-law and the observations in the low-velocity regime becomes obvious.

disturbances in the ambient radiation-driven stellar wind. Because of the large wavelength range of the HEROS spectra, the best-suited lines to follow these DACs in velocity and time could be carefully selected. Especially in some weak lines of Fe III and He I the observed DACs could be traced very precisely from photospheric velocities up to close to the terminal velocity of the stellar wind ($v_\infty \approx -350\,\mathrm{km\,s^{-1}}$). Figure 7 shows the measured acceleration of the absorption features through the ambient wind. It is interesting to note that the disturbances show almost a constant acceleration in the ambient stellar wind over a large velocity range from photospheric velocities up to the terminal velocity. If the observed velocity field of the absorption features is parameterized with a β-type velocity law as predicted by the radiation-driven wind theory for the homogeneous spherical symmetric wind, a value of $\beta = 2.5$ is needed to mimic the slow acceleration of the DACs. The velocity field for the ambient stationary homogeneous radiation-driven wind of ζ^1 Sco was derived by modeling the time-averaged P-Cygni Balmer profiles with a modified Sobolev Exact Integration (SEI) code by Lamers et al. (1987) and gives a faster acceleration with $\beta = 1.5$.

Basically two different models to explain the observed DACs exist: either we see a density enhancement due to a spherical symmetric thin shell ejected from the stellar surface and subsequently accelerated, or the density enhancement and therefore the absorption enhancement is caused by discrete patches of circumstellar material. These so-called "blobs" are also formed at the base of the wind and are accelerated in the line of sight towards the observer. Quasi-dynamical models based on these two scenarios

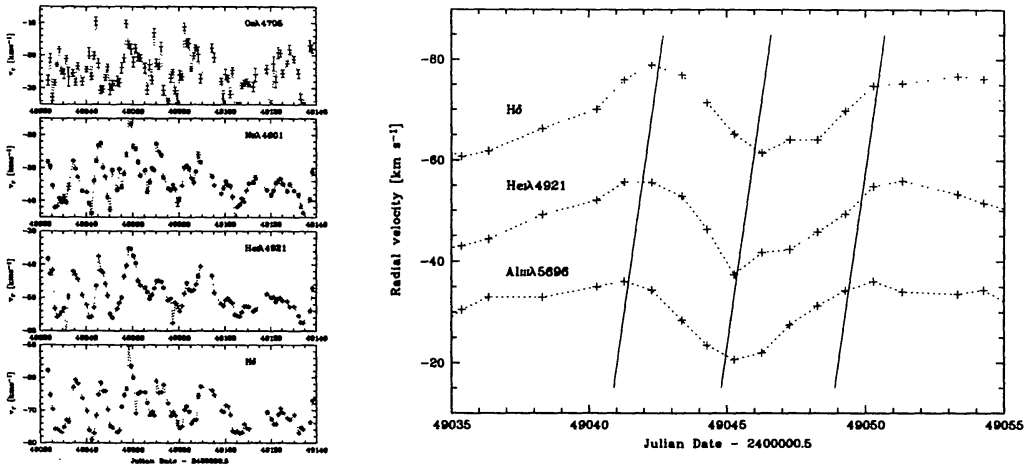

Figure 8: Left: pulsation-like radial-velocity variations of ζ^1 Sco as measured in 1993. Right: the velocity variations of the line centers; the sequence shows the shift in time *and* velocity of the pulsation pattern for Al IIIλ5696, He Iλ4921, and Hδ, i.e., in order of increasing height of formation in the non-hydrostatic photosphere.

allowed Rivinius et al. (1997a) to model the main characteristics of the observed dynamical spectra. The models assume that the wind variations, i.e., the DACs, are caused by density perturbations of the order of 10% at the base of the wind and are transported through the envelope according to the wind velocity law with $\beta = 2.5$. But interestingly it was found that only the "blob" model correctly accounts for the time development of both, the blue-shifted P-Cygni absorption with the DACs and the broad unshifted P-Cygni emission. The possibility to distinguish between these two scenarios can be qualitatively understood if the different contributions of an extended shell and of a localized blob to the P-Cygni emission are considered.

This leaves us with the following picture for the expanding envelope of ζ^1 Sco: a strong spherical-symmetric radiation-driven wind is structured by discrete blobs of enhanced density which originate close to the base of the wind and then slowly accelerate throughout the faster ambient wind.

Besides the wind-sensitive lines in the spectra of ζ^1 Sco, also a large number of photospheric lines is available for a detailed analysis of the photospheric variability and its possible relation to the variable envelope as described above. In Fig. 8 the radial-velocity curves measured for some representative photospheric lines are shown (left panel). The radial-velocity variations are pulsation-like with amplitudes of some $20\,\mathrm{km\,s^{-1}}$ and time scales of weeks – as already known from earlier observation from the seventies (cf. above). The really exciting new result from these time-series observations is that the intrinsically stable pulsation pattern appears with increasing time delays for increasing blue shift of the line center. The latter is to be identified with an increasing height of formation in the atmosphere already showing an outward accelerated expansion in photospheric layers. In other words: we see for the first time in a hot luminous star a pulsation-like disturbance originating in photospheric (or even sub-photospheric) layers traveling through the base of the stellar wind outwards into the expanding envelope.

The quite fixed pulsation pattern of many photospheric lines allows to use a cross-correlation technique to derive the delay times of many photospheric lines of different

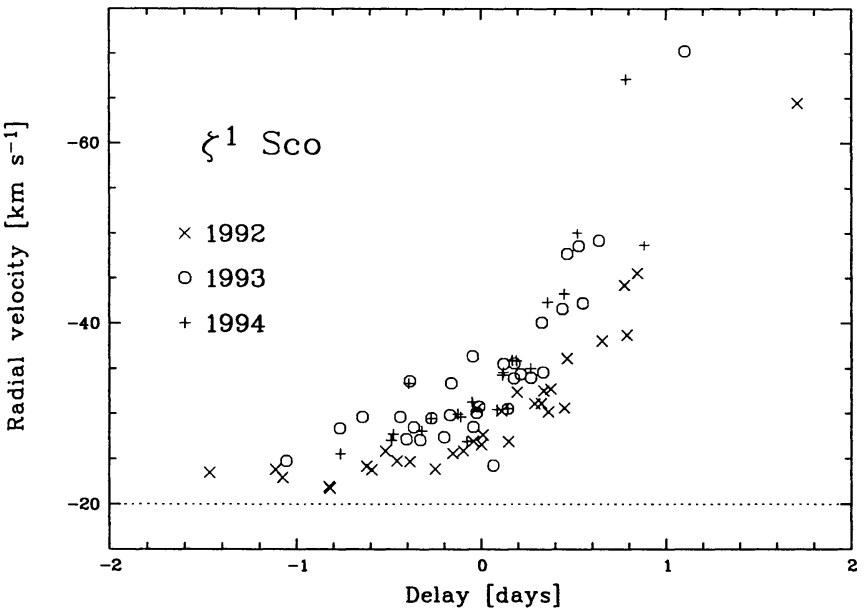

Figure 9: The propagation of disturbances in the cores of photospheric lines. The robustness of the cross-correlation method to derive this velocity law is demonstrated by the coincidence of the results derived from time series from different years. The dotted line indicates the systemic velocity of ζ^1 Sco.

depths of formation. In Fig. 9 the derived delay times are plotted versus the mean radial velocity of the respective line and therefore shows the expansion velocity field from the photosphere into the lower wind region with great detail.

With exception of the strongest DAC which was observed in 1993, it was not possible for Rivinius et al. (1997a) to causally connect the pulsation-like disturbances in photospheric layers at the base of the wind with the injection of the DACs. But a very general connection of the variability at the base of the wind to the variations found in the envelope is at least highly suggested by the observations.

5.3 The circumstellar and photospheric structures of late B- and early A-type supergiants[1]

The late B- and early A-type supergiants are evolved massive ($\approx 20\,M_\odot$) luminous ($\approx 10^5 L_\odot$) stars at the hot end of the transition zone between hot and cool supergiant stars. UV observations of resonance lines of singly ionized species indicate an accelerating outflow with terminal velocities of several hundred $\mathrm{km\,s^{-1}}$. This outflow is interpreted as a spherical symmetric mass loss due to a radiation-driven wind with typical mass-loss rates of $10^{-8}\,M_\odot \mathrm{yr}^{-1}$. The BA supergiants are well known to be photometrically and spectroscopically variable showing semiperiodic brightness and radial-velocity variations on time scales from days to several months (e.g. Burki 1978, Rosendhal 1970). In addition, timely unresolved peculiar variability of the wind-sensitive Hα line was observed which was early interpreted as variable mass loss and deviations of the spherical

[1]Based on the author's contribution to the ESO workshop on "Cyclic Variability in Stellar Winds" held in Garching, October 1997.

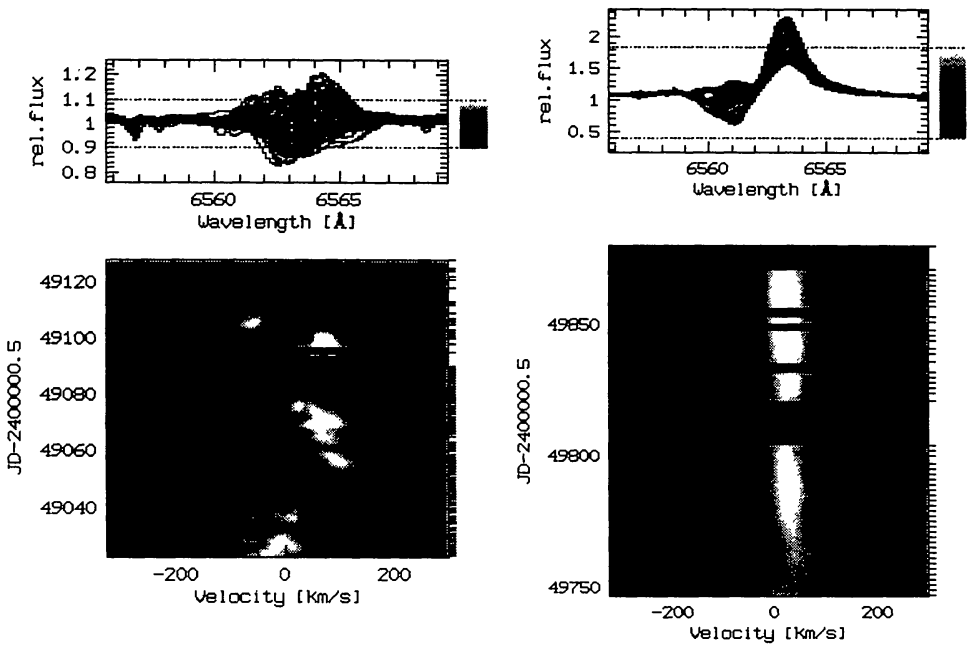

Figure 10: Dynamical Hα spectra of β Ori in 1993 (left) and HD 92207 in 1995 (right) showing the typical V/R variability caused by rotational modulation of the envelope.

symmetry of the envelope (Wolf & Sterken 1976).

The FLASH/HEROS data base contains a sample of six BA supergiants, i.e., HD 91619 (B7 Ia), HD 34085 (= β Ori = Rigel, B8 Ia), HD 96919 (B9 Ia), HD 92207 (A0 Ia), HD 100262 (A2 Ia), and HD 197345 (= α Cyg = Deneb, A2 Ia), which were observed in every year from 1993 to 1996 with about 100 spectra per object. Figure 10 shows dynamical spectra of the wind sensitive Hα line for two typical representatives of the BA supergiants: HD 92207 (A0 Ia, right) which in the timely average shows a distinct P Cygni-type wind profile indicating a strong radially accelerated outflow and β Ori (B8 Ia, left) where no clear P-Cyg profile is present but a photospheric absorption profile filled by wind emission roughly up to the continuum level. The crucial finding about the complex variability patterns is that – independent of the timely average appearance of the Hα profile – the variability is localized symmetrically about the system velocity with the maximum power of the variations just beyond the $\pm v \sin i$ velocities of the star (Kaufer et al. 1996a). The variations are mainly due to additional violet (V) and red (R) shifted emission components superimposed on the otherwise constant underlying wind or even photospheric profiles. This is clearly seen in the case of HD 92207 (Fig. 10, right) where the red P Cyg-emission peak is modulated in height and the blue shifted P Cyg absorption is filled with a blue-shifted emission peak of variable strength. The same type of V and R emission peak modulation is seen in β Ori (Fig. 10, left). The amplitudes of the modulations are measured for all program stars in the corresponding "temporal variance spectra" (TVS) and give equal amplitudes for the V and R peaks with values between 5% and 20% which are characteristic for the individual object. This characteristic V/R variability is highly indicative for deviations of the circumstellar envelopes of BA supergiants from spherical symmetry. Further – in analogy with the Be

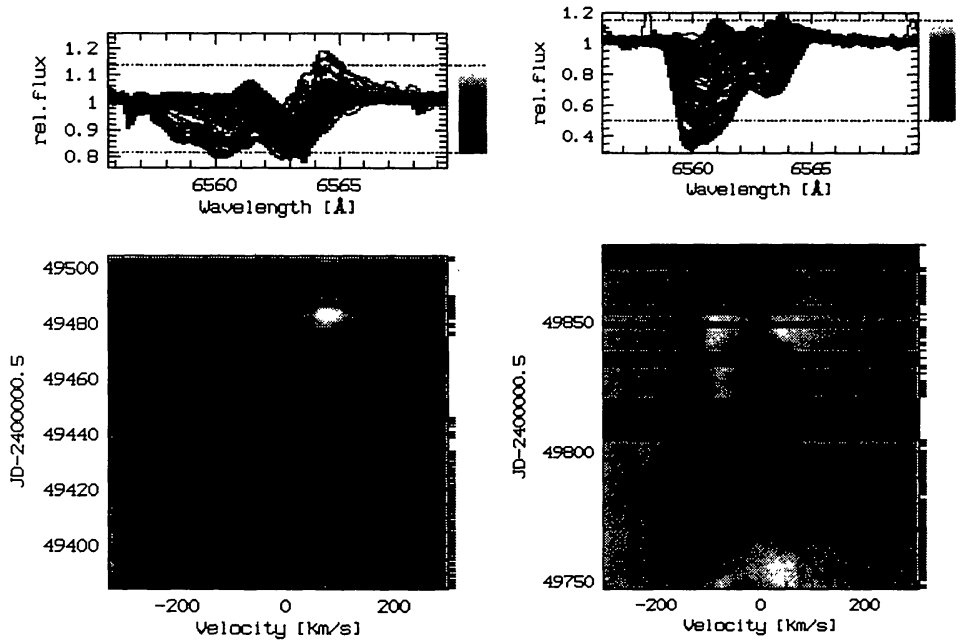

Figure 11: Dynamical Hα spectra of β Ori in 1994 (left) and HD 96919 in 1995 (right) showing the two best observed high-velocity absorption (HVA) events.

stars – this double-peaked emission variability suggests an equatorial concentration of the emitting circumstellar material.

The measured equivalent-width curves of the variable "excess" emission directly show the observed cyclical variability. A time-series analysis of the equivalent-width curves reveals for all examined stars basically *one* dominant period which is in all cases close to the rotational period estimated from the $v \sin i$. Therefore, rotational modulation of the lower circumstellar envelope by stellar surface structures is proposed as the major source of the observed Hα variability. An efficient coupling of the stellar rotation into the lower wind region could be provided by weak magnetic surface structures.

Further insight into the circumstellar structures in BA supergiants was obtained by the occasional observations of so-called "high-velocity absorptions" (HVA) which were for the first time identified an described in detail by Kaufer et al. (1996b). In Fig. 11 the two most prominent and so far best documented HVAs are shown as observed in the dynamical Hα spectra of β Ori (left) and HD 96919 (right). HVAs are described as suddenly appearing, extraordinarily deep, and highly blue- but also beyond $+v \sin i$ red-shifted absorptions in the circumstellar envelope. The appearance of the HVAs is announced either by V or $V + R$ emission peaks as known from the "normal" Hα variability. The sudden appearance of the blue shifted absorptions within a few days in the velocity range $v_{\rm sys} \rightarrow v_{\infty}$ is not compatible with the typical wind-flow times and therefore, the HVAs can *not* be explained as discrete mass-loss events at the base of the wind with a subsequent β-type acceleration of the "blob" within the ambient wind. In addition, the extreme depth of the absorptions suggests that the HVAs are caused by extended regions in the envelope which consist of dense and therefore probably recombined circumstellar structures. As a model to describe the observed HVAs, a rotating region of enhanced mass loss localized at the base of the wind near the stellar equator was proposed. The

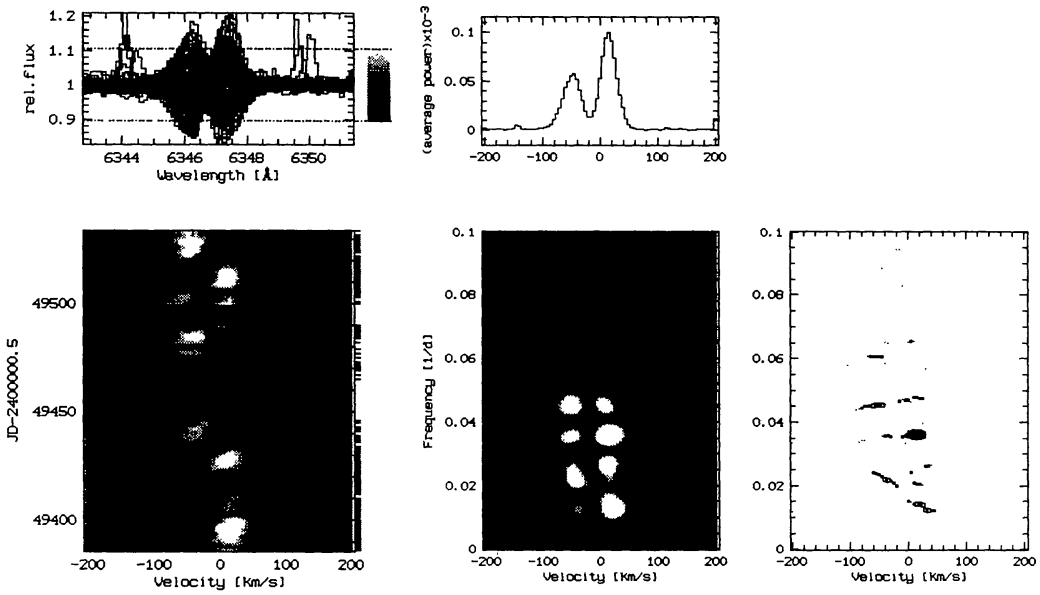

Figure 12: Left: dynamical spectrum of the photospheric SiIIλ6347 line (quotient with the mean spectrum) of HD 92207; middle: corresponding power spectrum; right: CLEANed periodogram, the estimated frequency of the radial fundamental pulsation is 0.05 days^{-1}.

continuously injected material is radially accelerated according to a slow β-type velocity law and due to the conservation of angular momentum builds up an extended rotating streak line in the equatorial plane of the envelope. This simple model primarily accounts for the sudden appearance of the HVA because the streak line rotates into the line of sight of the observer and the complete velocity field $v_{\rm sys} \rightarrow v_\infty$ becomes visible as extended and – since the observer looks along a large column of enhanced density – also deep absorption against the stellar disk. Assuming that the large streak-line structures are stable for at least a few stellar rotation cycles, this model predicts the reappearance of the HVA events after integer multiples of the stellar rotation period. For the case of the extreme HVA event in HD 96919 in 1995 the reappearance dates of the maximum blue absorption were predicted with the directly derived stellar rotation period of 93 days. And indeed, an HVA event with a strikingly similar time-velocity structure was observed during the 1996 HEROS run in La Silla – exactly after four rotational cycles.

Apart from the few optical lines sensitive to the circumstellar envelope, the HEROS wavelength range contains numerous metallic absorption lines of different strength and depth of formation. Therefore, these lines are well-suited to study the variability of the deeper photosphere but also the transition zone from the photosphere into the circumstellar envelope. By the use of an efficient cross-correlation technique the photospheric variability of the program stars was studied in subsets of the metallic lines with increasing depth of formation (Kaufer et al. 1997a). For all line groups, complex multiperiodic variations of the radial velocities with a typical velocity dispersion of 3 km s^{-1} were found. The CLEANed periodograms of these radial-velocity curves reveal for all program stars the excitation of multiple pulsation modes in accordance with the results found by Lucy (1976) for α Cyg. The photospheric period spectra are found to be clearly separated from the much longer rotation periods of the stars which rises the possibility to distinguish pulsation from rotation as source of the circumstellar variability. The fact

that the period spectra are not exactly reproducible from year to year heavily complicates any identification of the pulsation modes. The finding of periods longer and shorter than the estimated radial fundamental pulsation periods at least suggests the excitation of non-radial and radial overtone modes. A closer inspection of the photospheric LPVs of all studied stars shows occasionally prograde traveling features with crossing times over the profile considerably shorter than the estimated stellar rotation periods. These features are identified as azimuthally running non-radial pulsation patterns, most probably g-modes of low order ($\ell = |m| \leq 5$). Figure 12 illustrates the described photospheric variability showing the LPVs of the SiIIλ6347 line in HD 92207. The comparison of this photospheric variability pattern with the circumstellar variations in Fig. 10 (right panel) demonstrates the above mentioned separation of the respective time scales of the line profile variability. To date, no causal connection of this photospheric variability to the envelope's variability could be established, mainly due to the fact that both parts of the atmosphere show variability on very different time scales.

5.4 The outburst mechanism of the Be star μ Cen [2]

Most Be stars like μ Cen (HR 5193, B2 IV-Ve, $V = 2.9 - 3.5$ mag, $v \sin i = 130\,\mathrm{km\,s^{-1}}$) show short-periodic variability of the photospheric absorption-line profiles. On the other hand, the most enigmatic Be star activities are the apparently random line-emission outbursts probably associated with the building of a circumstellar Keplerian disk. μ Cen is one of the Be stars which shows the strongest and most frequent outbursts (Hanuschik et al. 1993). Although the idea of a causal connection of both phenomena is very attractive, all searches so far yielded negative results (e.g. Smith 1989).

Up to now, any significantly faster and stronger than average increase of the emission strength has been called an outburst. The large database built for this star with 409 FLASH and HEROS spectra from 355 nights allowed Rivinius et al. (1998b) now to give a general description of this phenomenon for μ Cen: an emission-line outburst is characterized by (i) a rapid rise and slow decline of circumstellar emission lines, (ii) a rapid appearance and slow decay of broad emission wings in hydrogen lines, (iii) a rapid increase and slow decrease of the emission-peak separation in optically thin lines, (iv) rapid intermittent

[2]Based on a the contribution of Th. Rivinius et al. to the proceedings of "A Half Century of Stellar Pulsation Interpretations" held in Los Alamos, June 1997, eds. P.A. Bradley & J.A. Guzik.

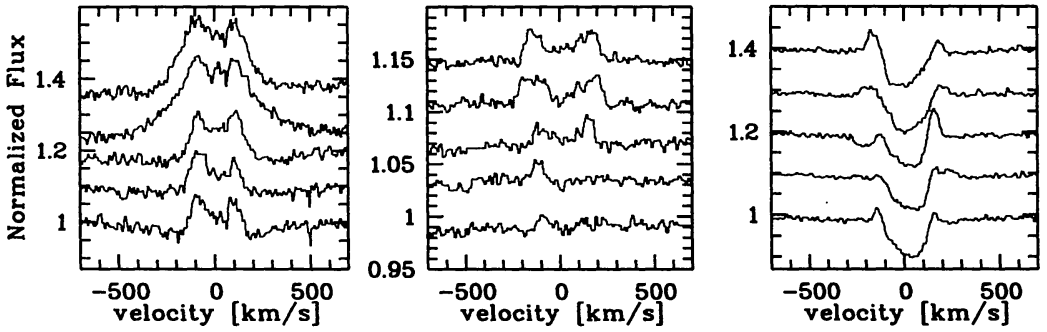

Figure 13: The evolution of an emission-line outburst in μ Cen over the course of 20 days (bottom to top, not equidistant in time) in Pa_{15} (left), SiIIλ6347 (middle), and HeIλ6678 (right).

Table 2: Parameters for the sinefits of the radial-velocity variability in the line cores of HeI$\lambda\lambda$4121,4168,4438

	Period $\mathcal{P}$ [days]	Phase ϕ at MJD=50 000	Amplitude A [km s^{-1}]
$\mathcal{P}_1$	0.502917 ± 0.000007	0.910 ± 0.011	15.3 ± 1.1
$\mathcal{P}_2$	0.507524 ± 0.000010	0.181 ± 0.016	8.1 ± 0.9
$\mathcal{P}_3$	0.494518 ± 0.000013	0.674 ± 0.025	5.1 ± 0.8
$\mathcal{P}_4$	0.281406 ± 0.000005	0.846 ± 0.021	7.6 ± 0.9

V/R variability of emission peaks. Examples of this behaviour are given in Fig. 13.

As shown by Fig. 13 (right) the HeIλ6678 line clearly displays low-order profile variability of the photospheric core which is indicative for non-radial pulsations in the star's photosphere. The radial velocities of lines least affected by emission were measured by fitting Gaussians to the cores of the HeI$\lambda\lambda$4121,4168,4438 lines. By applying Scargle's method (1982) in the range from 0-4 c/d and by iterative pre-whitening of the data with sinefits four periods were found (Table 2). The same values of $\mathcal{P}_1/\mathcal{P}_2/\mathcal{P}_3$ were derived from the analysis of the SiIII$\lambda\lambda$4553,4568 radial velocities, $\mathcal{P}_4$ was not detected in SiIII. So far only the radial-velocity data from 1992, 1995, and 1996 were used. However the variability patterns associated with these four periods are coherent over the whole time baseline, i.e., from 1992 to 1997. Three of these periods are closely spaced around the previously suspected 0.505 day period (Baade 1984). In fact, even in datasets covering as much as a year, the splitting would hardly be detectable. With only 0.28 days the fourth period is substantially shorter than the other three.

Radial velocities are (similarly to photometric data) a global, integrated quantity for which the information contained in the line profiles is underused by mixing it into just one number. In addition to the radial velocities, also the temporal flux variations were analyzed for several spectral lines as a function of the position within the line profile by applying the above mentioned prewhitening method to the intensity in $5\,\mathrm{km\,s^{-1}}$ wide velocity bins. A full description of the procedure is given in Kaufer et al. (1996a). Apart from the periods, which are fully consistent with the results from the radial-velocity data, this method also yields the power and phase distribution across the profile as plotted in Fig. 14, which in principle allows to determine the longitudinal and meridional quantum numbers (ℓ, m) of the non-radial pulsation modes of μ Cen.

The most striking feature is the basically identical behaviour with $\mathcal{P}_1$, $\mathcal{P}_2$, and $\mathcal{P}_3$. The phase difference from blue to red is $\Delta\phi \sim 1.6\pi$, which gives $\ell = 2$ using Telting & Schrijvers' (1997) Eq. [9]. The most probable value of m, based on the phase distributions, is -2. For $\mathcal{P}_4$ the same analysis gives $\ell = -m = 3$, i.e., the frequency of this variability is higher than the other three in both, time and space.

The splitting of the $\ell = 2$ group of periods is too small by at least one order of magnitude to be explained by rotational splitting. An explanation could rather be splitting due to different radial orders, n, of low-degree g-modes, which are indicated by the strongly double-peaked power distributions. In this case, however, the non-equidistant spacing of the periods remains to be explained.

Calculating the beating of $\mathcal{P}_1$, $\mathcal{P}_2$, and $\mathcal{P}_3$ it was found by Rivinius et al. (1997b) that the vectoral sum of the amplitudes is largest at times of the emission-line outbursts. Based

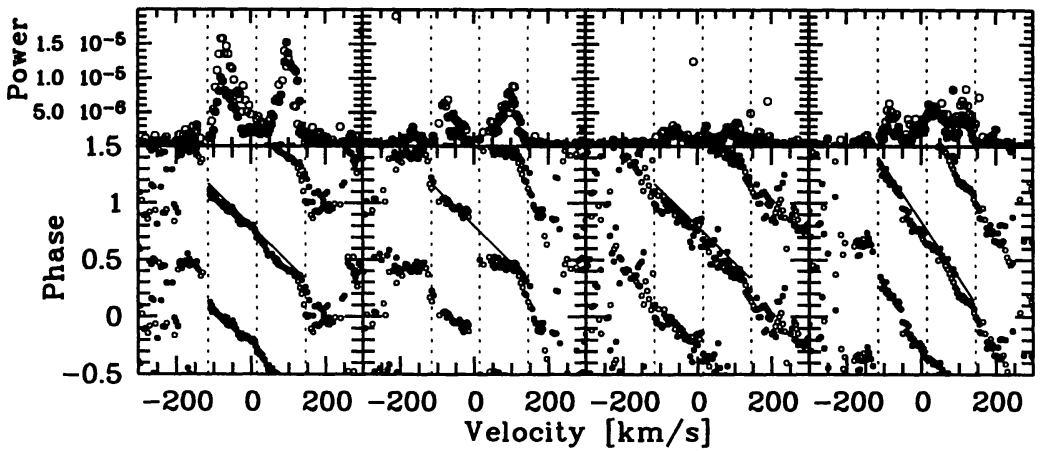

Figure 14: The phase diagrams of $\mathcal{P}_1$, $\mathcal{P}_2$, $\mathcal{P}_3$, and $\mathcal{P}_4$ (from left to right) for HeIλ4121 ($\bullet$) and HeIλ4713 ($\circ$). The three dotted lines mark the systemic velocity of $v_{\rm sys} = 14.5\,{\rm km\,s^{-1}}$, which was derived from the mean radial velocity of the SiIII$\lambda\lambda$4553,4568 lines, and $v_{\rm sys} \pm v \sin i$. The solid lines in the left three panels are the linear regression of the phase with velocity computed for $\mathcal{P}_1$ only (in order to stress the similar behaviour of these three periods), whereas in the rightmost panel the $\mathcal{P}_4$ data are used.

on this, a purely empirical model to predict the times of the outbursts was constructed, in which no assumptions about the underlying physical processes are made. Its main properties are that the amplitudes of the individual periods are permitted to grow between outbursts and, when the overall amplitude exceeds a certain threshold, mass is transferred into the circumstellar disk and the individual pulsation amplitudes are damped. This crude model also gives an estimate of the strength of the outburst.

With this model it is possible to reproduce the times of the outbursts covered by the FLASH/HEROS database to within a week. The *same set* of parameters describes the Hα outbursts observed in 1987 by Hanuschik et al. (1993) with the same accuracy (Fig. 15). In addition, forthcoming outbursts for 1997 were predicted by Rivinius et al. (1997b) and indeed confirmed by subsequent observations as recently reported by Rivinius et al. (1998a).

The multiperiodicity of the stellar radial-velocity variations, the connected line-profile variations, and the shapes and widths of the phase and power distributions of μ Cen led to the identification of four coherent non-radial pulsation modes. All of them are likely to be low-order g-modes. Three of these modes are very closely spaced and have identical angular indices of $\ell = -m = 2$, the fourth one has $\ell = -m = 3$. The very small spacing of the first three modes of this rapidly rotating star suggests that they are due to different radial orders n. Since only three modes contribute significantly to the beating model for the line-emission outbursts, little room remains for other modes with significant amplitude (i.e., $> 5\,{\rm km\,s^{-1}}$). The density of the g-eigenmode spectrum of B-type stars in this range therefore requires an effective selection mechanism. Since the observed period spacing is not equidistant, either there are unexcited/damped modes or the spacing deviates significantly from an equidistant scheme.

The most striking finding is that from the analysis of the purely photospheric line-profile variability it was possible to derive the circumstellar variability pattern. This is strongly mutually assuring of the reliability of the time series analyses of stellar and

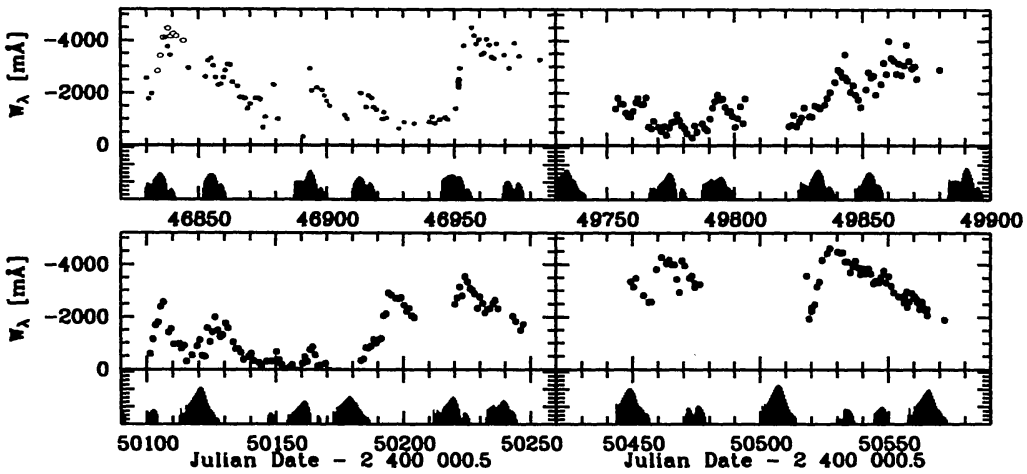

Figure 15: The observed emission equivalent width (upper parts of the panels) and the calculated mass transfer to the disk in arbitrary units (lower parts of the panels). The 1987 data of Hα (upper left) was observed by Hanuschik et al. (1993), while for 1995 (upper right), 1996 (lower left), and 1997 (lower right) the Pa_{15} data is shown.

circumstellar lines. More importantly, it demonstrates for the first time that the outbursts of Be stars may really be causally connected to their photospheric low-order line profile variability. A simple model based on the beating of the photospheric multiperiodicity is able to reproduce the epochs, partly also the strengths, of outbursts over a full decade. Non-radial pulsation can, therefore, be a (contributing) driver of episodic mass loss from Be stars.

6 Conclusions

The above reported astronomical results of eight years of intense spectroscopic monitoring of different classes of luminous hot stars with high resolution in wavelength and time impressively demonstrate the importance and potential impact of long-term monitoring campaigns for the studies of stellar atmospheres' variability. Particularly the first conclusive results on the physical connection between the variability of the stellar photospheres and the variability of the envelopes as found in ζ^1 Sco and μ Cen are extremely promising for a further deeper understanding of the involved physical mechanisms acting in there.

An important conclusion of this work could be, that in an era of $8-16$-m telescopes highly exciting and fundamental astronomical research can be done even with small to medium-size telescopes – if they are equipped with up-to-date instruments and dedicated observing programs. In this context it is worth to note that the European Southern Observatory recently funded a new state-of-the-art high-resolution spectrograph named FEROS for the ESO 1.52-m telescope on La Silla, which is built by an European consortium under the leadership of the Landessternwarte Heidelberg (cf. Kaufer et al. 1997b).

Acknowledgements

First, I would like to thank the PIs of the FLASH/HEROS long-term program, namely B. Wolf and

O. Stahl who initiated and very actively supported this project with their continuous comittment and apparently inexhaustible experience. Further, this project fundamentally relies on the careful work and patience of the observers who spent many nights at the telescopes, namely, D. Baade, Th. Dumm, Th. Gäng, C.A. Gummersbach, H. Henrichs, I. Jankovics, J. Kovács, H. Lehmann, H. Mandel, J. Peitz, Th. Rivinius, D. Schäfer, W. Schmutz, J. Schweickhardt, O. Stahl, S. Štefl, N. Stumpf, Th. Szeifert, U. Thiel, and B. Wolf. We all thank the European Southern Observatory for generous allocation of observing time and the staff at La Silla for the kind assistance during the observations. This work is financially supported by the Deutsche Forschungsgemeinschaft (Wo296/16-1,2, Wo296/20-1, Ap16/6-1).

References

Baade D., 1984, A&A **135**, 101
Babel, J., Montmerle, T., 1997, Apj **485**, L29
Burki G., 1978, A&A **65**, 357
Conti P., 1972, ApJ **174**, L79
Gagné M., Caillaut J.-P., Stauffer J.R., Linsky, J.L., 1997, Apj **478**, L87
Hanuschik R.W., et al., 1993, A&A, **274**, 356
Kaufer A., Stahl O., Wolf B., et al., 1996a, A&A **305**, 887
Kaufer A., Stahl O., Wolf B., et al., 1996b, A&A **314**, 599
Kaufer A., Stahl O., Wolf B., et al., 1997a, A&A **320**, 273
Kaufer A., Wolf B., Andersen J., Pasquini L., 1997b, The ESO Messenger **89**, 1
Lamers H.J.G.L.M., Cerruti-Sola M., Perinotto M., 1987, ApJ **314**, 726
Lucy L.B., 1976, ApJ **206**, 499
Mandel H., 1988, High-resolution spectroscopy with a fiber-linked echelle spectrograph. In: Cayrel de Strobel G., Spite M. (eds.), IAU Symp. **132**, Kluwer, p. 9
Rivinius Th., Stahl O., Wolf B., et al., 1997a, A&A **318**, 819
Rivinius Th., Baade D., Štefl S., et al., 1997b, Be star Newsletter **32**, 14
Rivinius Th., Baade D., Štefl S., et al., 1998a, In: proceedings of the ESO workshop on "Cyclic Variability in Stellar Winds" held in Garching, October 1997, in press
Rivinius Th., Baade D., Štefl S., et al., 1998b, submitted to A&A
Rosendhal J.D., 1970, ApJ **159**, 107
Scargle J.D., 1982, ApJ **263**, 835
Smith M.A., 1989, ApJS **71**, 357
Stahl O., Wolf B., Gäng Th., et al. , 1993, A&A **274**, L29
Stahl O., Wolf B., Gäng Th., et al., 1994, A&AS **107**, 1
Stahl O., Kaufer A., Wolf B., et al., 1995, The Journal of Astronomical Data **1**, 3 (published on CD-ROM)
Stahl O., Kaufer A., Rivinius Th., et al. , 1996, A&A **312**, 539
Sterken C., 1977, A&A **57**, 361
Sterken C., Wolf B., 1978, A&A **70**, 641
Telting J., Schrijvers C., 1997, A&A **317**, 723
Walborn N.R., 1981, ApJ **243**, L37
Wolf B., Sterken C., 1976, A&A **53**, 355
Wolf B., Appenzeller I., 1979, A&A **78**, 15
Wolf B., Mandel H., Stahl O., et al., The ESO Messenger **74**, 19